NMR Solution Structure of an Oligonucleotide Hairpin with a 2′F-ANA/RNA Stem: Implications for RNase H Specificity toward DNA/RNA Hybrid Duplexes

Jean-François Trempe,[‡] Christopher J. Wilds,[§,||] Alexei Yu. Denisov,[‡] Richard T. Pon,[⊥] Masad J. Damha,*[,§] and Kalle Gehring[‡,§]

Department of Biochemistry and Montreal Joint Center for Structural Biology, McGill University, Montreal, Canada, Department of Chemistry, McGill University, Montreal, Canada, and University Core DNA Services, The University of Calgary, Canada

Received November 2, 2000

Abstract: The first structure of a 2′-deoxy-2′-fluoro-D-arabinose nucleic acid (2′F-ANA)/RNA duplex is presented. We report the structural characterization by NMR spectroscopy of a small hybrid hairpin, r(GGAC)-d(TTCG)2′F-a(GTCC), containing a 2′F-ANA/RNA stem and a four-residue DNA loop. Complete ^{1}H, ^{13}C, ^{19}F, and ^{31}P resonance assignments, scalar coupling constants, and NOE constraints were obtained from homonuclear and heteronuclear 2D spectra. In the chimeric duplex, the RNA strand adopts a classic A-form structure having C3′ endo sugar puckers. The 2′F-ANA strand is neither A-form nor B-form and contains O4′ endo sugar puckers. This contrasts strongly with the dynamic sugar conformations previously observed in the DNA strands of DNA/RNA hybrid duplexes. Structural parameters for the duplex, such as minor groove width, *x*-displacement, and inclination, were intermediate between those of A-form and B-form duplexes and similar to those of DNA/RNA duplexes. These results rationalize the enhanced stability of 2′F-ANA/RNA duplexes and their ability to elicit RNase H activity. The results are relevant for the design of new antisense drugs based on sugar-modified nucleic acids.

Introduction

The ability of oligonucleotides to form a duplex with a particular RNA species enables specific control of gene expression.[1] This approach, referred to as antisense strategy, is becoming increasingly important in therapeutic strategies against a range of human diseases, including cancer and infectious diseases. Phosphorothioate oligodeoxynucleotides (S-DNA), developed as first-generation antisense agents, have progressed to late-stage clinical development, and one compound has received FDA approval.[2] These compounds are thought to operate primarily by sequence-specific binding to the targeted RNA. The resultant hybrid heteroduplex recruits RNase H, an ubiquitous endonucleolytic enzyme that cleaves the targeted RNA strand.[3,4]

The origins of the substrate specificity of RNase H are not fully understood at present. Although RNase H cleaves only the RNA strand of the hybrid, this action is dependent on the chemical nature of the opposite strand in the hybrid duplex. For example, *Escherichia coli* RNase H binds to duplex RNA but cannot cleave it.[5] Similarly, hybrids in which the antisense strand is phosphoramidate DNA, 2′-OMe RNA, or 2′F-RNA, to name a few, are not substrates of RNase H.[2] The development of antisense compounds that are able to induce cleavage in hybrid duplexes is of intense interest. One such class of compounds is nucleic acids composed of 2′-deoxy-2′-fluoro-D-arabinose residues (2′F-ANA; Figure 1a). 2′F-ANA/RNA

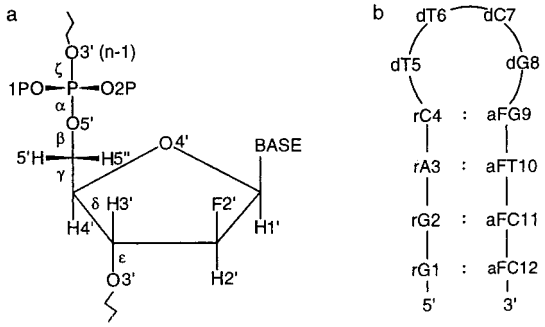

Figure 1. Chemical structures. (a) Stereochemical nomenclature of a 2′F-arabinonucleotide (2′F-ANA). The naming of the atoms and backbone torsion angles are shown for the fluoroarabinose ring and phosphodiester backbone. In 2′F-arabinose, the 2′ fluorine atom is above the ring (β), as opposed to ribose in which the 2′ hydroxyl group is below. (b) Secondary structure of the chimeric hairpin: residues 1−4 are ribonucleotides (rX), residues 5−8 are deoxyribonucleotides (dX), and residues 8−12 are 2′F-arabinonucleotides (aF-X).

* To whom correspondence should be addressed: Masad J. Damha, Department of Chemistry, Otto Maass Chemistry Building, 801 Sherbrooke Street West, Montreal, QC, H3A 2K6, Canada. E-mail: masad.damha@mcgill.ca

‡ Department of Biochemistry and Montreal Joint Center for Structural Biology, McGill University.

§ Department of Chemistry, McGill University.

⊥ University Core DNA Services, The University of Calgary.

|| Current address: Department of Biological Sciences, Vanderbilt University, Nashville, TN 37235.

(1) Stephenson, M. L.; Zamenick, P. C. *Proc. Natl. Acad. Sci. U.S.A.* **1978**, *75*, 285−288.

(2) Cook, P. D. *Second Generation Antisense Oligonucleotides: 2′-Modifications*; Bristol, J. A., Ed.; Academic Press: San Diego, CA, 1998; Vol. 33, pp 313−325.

(3) Walder, R. Y.; Walder, J. A. *Proc. Natl. Acad. Sci. U.S.A.*, **1988**, *85*, 5011−5015.

(4) Monia, B. P.; Lesnik, E. A.; Gonzalez, C.; Lima, W. F.; McGee, D.; Guinosso, C. J.; Kawasaki, A. M.; Cook, P. D.; Freier, S. M. *J. Biol. Chem.* **1993**, *268*, 14514−14522.

(5) Lima, W. F.; Crooke, S. T. *Biochemistry* **1997**, *36*, 390−398.

10.1021/ja003859p CCC: $20.00
Published on Web 05/04/2001

hybrid duplexes invoke RNase H activity and have enhanced thermal stability, as compared to DNA/RNA duplexes.[6]

NMR studies on DNA/RNA hybrid duplexes have shown that their global conformation is distinct from A- and B-form of DNA and has often been termed H-form.[7−14] The RNA strand shows A-type helical features, and the DNA strand shows an intermediate conformation between that of A- and B-DNA. On the basis of measurements of interproton distances, Reid and co-workers proposed an O4′ endo configuration for the DNA sugar moieties.[8,10,12] Other studies, based on measurements of scalar couplings, suggested that the DNA strand rapidly exchanges between C2′ endo and C3′ endo conformers.[9,11,13,14] Despite these differences in interpretation of NOE and scalar coupling data, the hybrid DNA/RNA duplex structures show similar helical parameters. Notably, the minor groove width is slightly narrower in hybrid duplexes than in RNA duplexes; this is believed to be important for RNase H recognition of the hybrid duplex.[8,9,12−15]

Chemical modification of the sugar ring strongly affects sugar puckering and the overall structure of the nucleic acid. Berger et al.[16] have reported the crystal structure of a B-DNA duplex having two 2′F-arabinonucleotides and observed the O4′ endo puckering for these residues in the context of an overall B-form duplex. They also observed that the stability of the duplex was enhanced by the 2′F-ANA residues. The strong gauche effect between the highly electronegative fluorine atom and the O4′ oxygen,[17−19] as well as steric effects,[16] have been suggested to lock the five-membered ring into the O4′ endo sugar pucker, mimicking the average deoxyribose conformation in hybrid duplexes. More recently, two groups independently modeled 2′F-ANA/RNA hybrid duplexes, using either the X-ray structure of a DNA duplex with [3.3.0]bicycloarabinose (T) nucleotides that adopt an O4′ endo conformation[20] or by solely computational methods.[21] Both studies suggest that a hybrid duplex with O4′ endo sugar puckering in one strand would adopt a structure with averaged A-form and B-form structural parameters.

We report here the first solution structure of a hybrid 2′F-ANA/RNA duplex. The duplex is part of a small chimeric hairpin containing RNA, DNA, and 2′F-ANA residues (Figure 1b). The reason for the choice of this particular sequence was that the analogous all-RNA and all-DNA hairpins had A-form and B-form structures, respectively.[22,23] In addition, the DNA loop is relatively flexible and has little influence on the stem conformation.[23] We find that the 2′F-ANA/RNA stem is structurally very similar to a DNA/RNA hybrid duplex. The minor groove width is intermediate, and the 2′F-ANA residues adopt the O4′ endo conformation. These results suggest that 2′F-ANA/RNA acts as a substrate for RNase H by structural mimicry of DNA/RNA hybrid duplexes with the increased stability due to structural preorganization of the 2′F-ANA strand.

Experimental Section

Sample Preparation. Synthesis of r(GGAC)d(TTCG)2′F-a(GTCC) was carried out following modifications of our literature procedure.[19] A PE/Biosystems 394 four-column, 8-base DNA synthesizer was configured with the 2′F-arabinose and 2′-deoxyribose nucleoside phosphoramidites (0.1 M). Four 1-mmol scale synthesis columns containing the 3′ terminal 2′F-araC were installed, and the first eight bases were synthesized, that is, d(TTCG)2′F-a(GTCC). The 2′F-arabinonucleosides were replaced with 2′-ribose nucleoside phosphoramidites (0.1 M), and the synthesis was completed. All of the coupling steps were performed using a 1-μmol-scale RNA coupling cycle (10 min coupling) and 3-(ethylthio)-1H-tetrazole (0.75 M, American International Chemical; Natick, MA). A trityl-off/manual ending was performed.

The controlled-pore glass (CPG) support was removed from the columns, placed in screw-capped glass tubes, and heated in saturated methanolic ammonia (16 h, 55 °C). The methanol was removed, transferred to a polystyrene tube (5 mL), and evaporated to dryness. The residue was suspended in neat triethylamine−trihydrofluoride (0.5 mL) and stirred overnight. Water (3 mL) was added, the solutions were evaporated to a thick oil, redissolved in water (1 mL), and desalted on an NAP-10 prepacked Sephadex column (total yield, 188 A_{260} units).

Anion-exchange HPLC purification was performed on a Waters DEAE-5PW preparative column (22.5 × 150 mm) at 50 °C using aqueous sodium perchlorate gradient (5 mL/min). Product peak fractions were combined, concentrated, and desalted on Sephadex G-25 (total yield, 59 A_{260} units).

The melting point of the hairpin was found to be 67 °C, as determined from UV melting curves at 260 nm.[24] The melting point was also determined for r(GGAC)d(TTCGGTCC).[24] As expected, the melting point was lower, that is, 60 °C. Incorporation of 2′F-arabinonucleotides increases the thermodynamic stability of the hybrid duplex, as compared to the natural DNA/RNA duplex.[6,19]

NMR Spectroscopy. Proton and phosphorus spectra were recorded on a Bruker DRX 500 equipped with a $^{1}H/^{13}C/^{31}P$ triple resonance *x*, *y*, *z* gradient probe. The $^{1}H-^{19}F$ HETCOR was recorded on a Bruker DRX 300 equipped with a $^{1}H/^{13}C/^{31}P/^{19}F$ quadruple resonance probe. Sample concentration was 0.5 mM in either 90% H_2O/10% D_2O (for imino spectra) or 100% D_2O, pH 7.2. ^{1}H resonances were referenced internally to DSS. Phosphorus and fluorine resonances were indirectly referenced to H_3PO_4 (85%) (0 ppm ^{31}P) and trifluoroacetic acid (0 ppm ^{19}F) by multiplying the DSS proton frequency by 0.404807356 or 0.940866982, respectively.[25] All 2D spectra in D_2O were collected using TPPI and presaturation of the residual HDO signal.

A 2D NOESY in H_2O was collected at 278 K using a jump-return pulse sequence and a mixing time of 179 ms. A series of NOESY spectra in D_2O were collected at mixing times of 50, 200, and 400 ms at 293 K. A double-quantum filtered COSY (DQF−COSY) was

(6) Damha, M. J.; Wilds, C. J.; Noronha, A.; Brukner, I.; Borkow, G.; Arion, D.; Parniak, M. A. *J. Am. Chem. Soc.* **1998**, *120*, 12976−12977.
(7) Chou, S. H.; Flynn, P.; Reid, B. *Biochemistry* **1989**, *28*, 2435−2443.
(8) Fedoroff, O.; Salazar, M.; Reid, B. R. *J. Mol. Biol.* **1993**, *233*, 509−523.
(9) Lane, A. N.; Ebel, S.; Brown, T. *Eur. J. Biochem.* **1993**, *215*, 297−306.
(10) Salazar, M.; Fedoroff, O. Y.; Miller, J. M.; Ribeiro, N. S.; Reid, B. R. *Biochemistry* **1993**, *32*, 4207−4215.
(11) González, C.; Stec, W.; Reynolds, M. A.; James, T. L. *Biochemistry* **1995**, *34*, 4969−4982.
(12) Fedoroff, O. Y.; Ge, Y.; Reid, B. R. *J. Mol. Biol.* **1997**, *269*, 225−239.
(13) Gyi, J. I.; Lane, A. N.; Conn, G. L.; Brown, T. *Biochemistry* **1998**, *37*, 73−80.
(14) Bachelin, M.; Hessler, G.; Kurz, G.; Hacia, J. G.; Dervan, P. B.; Kessler, H. *Nature Struct. Biol.* **1998**, *5*, 271−276.
(15) Horton, N. C.; Finzel, B. C. *J. Mol. Biol.* **1996**, *264*, 521−533.
(16) Berger, I.; Tereshko, V.; Ikeda, H.; Marquez, V. E.; Egli, M. *Nucleic Acids Res.* **1998**, *26*, 2473−2480.
(17) Damha, M. J.; Pon, R. T.; Gehring, K.; Wilds, C. J.; Lok, C.; Noronha, A. M.; Viazovkina, E. V.; Parniak, M. A. Physicochemical and biological properties of arabinonucleic acids (ANA and 2′F-ANA). In *Carbohydrate-Based Ligands Targetting Nucleic Acids*, 218th American Chemical Society, National Meeting & Exposition, New Orleans, LA, 1999.
(18) Lok, C.-N.; Viazovkina, K.; Wilds, C. J.; Noronha, A. M.; Trempe, J.-F.; Denisov, A.; Pon, R. T.; Parniak, M. A.; Gehring, K.; Damha, M. J. Antisense Properties of Arabinonucleic Acids & NMR Solution Structure of 2′F-ANA/RNA and ANA/RNA Hybrids; XIV International Roundtable on Nucleosides, Nucleotides and Their Biological Applications: San Francisco, CA, 2000.
(19) Wilds, C. J.; Damha, M. J. *Nucleic Acids Res.* **2000**, *28*, 3625−3635.
(20) Minasov, M.; Teplova, M.; Nielsen, P.; Wengel, J.; Egli, M. *Biochemistry* **2000**, *39*, 3525−3532.
(21) Venkateswarlu, D.; Ferguson, D. M. *J. Am. Chem. Soc.* **1999**, *121*, 5609−5610.
(22) Varani, G.; Cheong, C.; Tinoco, I. J. *Biochemistry* **1991**, *30*, 3280−3289.
(23) James, J. K.; Tinoco, I. J. *Nucleic Acids Res.* **1993**, *21*, 3287−3293.
(24) Wilds, C. Ph.D. Thesis, ″McGill University: Montreal, QC, 1999.
(25) Maurer, T.; Kalbitzer, H. R. *J. Magn. Reson. Series B* **1996**, *113*, 177−178.

Table 1. Scalar Coupling Constants in Hz[a] and Pseudorotation Analysis of Sugar Puckers[b]

	1′2′	1′2″	2′3′	2″3′	3′4′	4′5′ + 4′5″	3′P	f_1, %	P_1	P_2
rG1	<2	−[c]	5.0	−	9.0	6.0	10	100	18−44	−
rG2	<2	−	4.0	−	9.5	5.0	9	100	9−39	−
rA3	<2	−	n.d.[d]	−	n.d.	n.d.	9	n.d.	n.d.	n.d.
rC4	3.0	−	4.0	−	8.0	4.0	9	100	31−52	−
dT5	5.5	7.5	6.5	6.0	5.5	6.0	5	56−74	10−44	150−177
dT6	10.0	5.5	7.5	<2	2.5	6.0	6	92−100	127−146	25−43
dC7	9.0	5.5	7.0	2.5	3.0	6.5	5	81−87	125−164	6−55
dG8	10.0	5.5	6.2	2.2	2.9	8.5	3	92−100	138−151	4−36
aFG9	3.8	−	<2	−	6.2	6.0	4	80−100	73−110	153−167
aFT10	4.2	−	<2	−	6.0	4.5	4	72−100	75−115	133−177
aFC11	4.0	−	<2	−	5.8	5.0	4	86−100	77−109	138−168
aFC12	4.2	−	3.3	−	6.0	5.0	−	42−53	94−120	8−37

[a] Uncertainties are ±0.5 Hz for 1′2′ and 1′2″ couplings, ±1 Hz for other homonuclear couplings, and ±2 Hz for 3′P. [b] Molar fraction (%) of conformer 1 and phase angle of conformers 1 and 2 were calculated using the program PSEUROT. Minimum and maximum values are shown for each data set. [c] −, not applicable. [d] Not determined.

recorded at 293 K with 4 K points in t_2 and 1 K in t_1. Data were zero-filled to 8 K in t_2 and 2 K in t_1, resulting in a resolution of 0.5 Hz in t_2 and 2 Hz in t_1. A DQF−COSY with broadband phosphorus decoupling was recorded under the same acquisition and processing conditions.

The chemical-shift dispersion in the sugar protons region was favorable for assignments and coupling measurements. Well-established sequential assignment techniques[26] were used to assign H1′ and base protons. Most of the NOE peaks were well-resolved, except for peaks near the diagonal in the 4−5 ppm region of the spectrum. Stereospecific assignments were obtained for some stem residues H5′/H5″ based on H3′−H5′/5″ NOE intensities, assuming a gauche$^+$ γ torsion angle. Heteronuclear correlation spectra (^{1}H−^{31}P and ^{19}F−^{1}H HETCOR) were used to assign phosphorus and fluorine resonances.

NMR Restraints. Distance restraints were derived from NOESY spectra at mixing times of 50 and 200 ms using the r^{-6} distance relationship. NOE intensities were evaluated by integrating directly cross-peaks in the NOESY spectra. To account for the differences in cross-relaxation rates, 2 calibrations were done: one for the stem (based on the aF-C11 H5−H6 NOE) and one for the loop (dC7 H5−H6), assuming a distance of 2.46 Å between H5 and H6.

Distance constraint error bounds were evaluated as following. Vicinal protons distances were given a narrow ±0.2 Å error bound. All other distances in the stem were given 10% lower error bounds and 20−30% upper error bounds. Because of an absence of a single conformation and a high mobility in the loop, larger error bounds (50−100%) were given to distance constraints in the loop. A total of 210 distance constraints were used for calculations: 98 (59 in stem) intraresidue NOE-derived, 94 (61 in stem) sequential NOE-derived, 3 (1 in stem) long-range NOE-derived ,and 15 for hydrogen bonds in the stem.

Proton $J_{1'2'}$ and $J_{1'2''}$ were measured directly from peak splitting in the $\omega 2$ frequency domain of DQF−COSY using phosphorus decoupling, and other couplings were extracted from sums of couplings and then were used to calculate coupling constants, as previously described.[27] Line widths were ∼3 to 4 Hz. The coupling constants were then validated by comparing values obtained to relative peak intensities. Coupling constants are shown in Table 1. ^{1}H−^{9}F coupling constants (^2J and ^3J) were measured from fluoroarabinonucleotides 1′-2′ and 2′-3′ cross-peaks in NOESY and DQF−COSY spectra. ^{1}H−^{19}F ^5J between base protons and intraresidue fluorine was also measured from NOE peaks' splitting. Heteronuclear ^{1}H−^{19}F coupling constants are shown in Table 2. The computer program PSEUROT[28,29] was used to estimate phase angles of pseudorotation from coupling constants using standard electronegativities and orientation terms and assuming a fixed puckering amplitude of 37°. Maximum and minimum values were calculated according to uncertainties in coupling constant measurements. Results of PSEUROT calculations are shown in Table 1.

Table 2. ^{1}H−^{19}F Scalar Coupling Constants in Hz[a]

	1′F	2′F	3′F	6/8-F
aFG9	22.5	49.8	21.3	2.7
aFT10	22.8	52.1	26.8	1.5
aFC11	21.0	52.8	26.8	1.5
aFC12	19.1	54.5	25.1	1.7

[a] Uncertainty is ±0.5 Hz for all measurements.

β- and ϵ-angle restraints were derived from P−H3′ and P−H5′/H5″ coupling constants, respectively. The P−H3′ coupling constant was obtained by measuring the difference in $\sum J_{H3'}$ for cross-peaks in DQF−COSY with and without phosphorus decoupling. P−H5′/H5″ was estimated qualitatively from the ^{1}H−^{31}P HETCOR spectrum. γ-torsion angles were estimated from sums of H4′−H5′ and H4′−H5″ coupling constants.

Ninety-one dihedral angle constraints (61 in stem) were determined from coupling constant analysis. β-angles were given a ±40° error for stem residues and ±60° in the loop. γ-angles were given a ±30°error for stem residues and ±60° in the loop. ϵ-angles were given a ±20° error for stem residues and ±100° in the loop. All of the sugar torsion angles that define pseudorotation phase angles were given a ±10°error.

Molecular Modeling. The X-PLOR package, version 3.843,[30] was used to calculate the nucleic acid hairpin structures. The nucleic acid all-hydrogen force field of X-PLOR (parallhdg.dna) was modified to include parameters for the fluorine atoms: C−F bond length, bond angles, dihedral terms, improper angles, charges, van der Waals radius, and polarizability.[21,31]

A set of 10 random coordinate files was initially generated for the structure calculation by simulated annealing without experimental constraints.[32] NMR constraints were added, and simulated annealing at 15 000 K for 5 ps was used to generate 15 structures from each random coordinate file. Of the structures, 68 out of the 150 had total energy <1000 kcal/mol. The RMSD of low-energy structures originating from the same starting conformation was not significantly different from the RMSD of low-energy structures originating from different conformations. Five structures with the smallest number of experimental restraint violations were then submitted to another simulated annealing step at 5000 K for 3 ps to reduce the number of violations before the last refinement step. Previously described refinement steps were performed using a constant repel-only r^2 van der Waals energy term and no electrical term. Gentle refinement was accomplished from each of these 5 structures using 10 ps of simulated annealing starting from an annealing temperature of 300 K. Force constants for

(26) Wüthrich, K. *NMR of Proteins and Nucleic Acids*; John Wiley & Sons: New York, 1986.

(27) Wijk, J. v.; Huckriede, B. D.; Ippel, J. H.; Altona, C. *Methods Enzymol.* **1992**, *211*, 286−304.

(28) de Leeuw, F. A. A. M.; Altona, C. *QCPE 463: PSEUROT 3B*; Quantum Chemistry Program Exchange, Indiana University: Bloomington, IN, 1983.

(29) Rinkel, L. J.; Altona, C. *J. Biomol. Struct. Dyn.* **1987**, *4*, 621−649.

(30) Brünger, A. T. *X-Plor 3.1, a System for X-ray Crystallography and NMR*; Yale University Press: New Haven, CT, 1992.

(31) Isaacs, N. *Physical Organic Chemistry*, 2nd ed.; Longman Scientific and Technical: New York, 1995.

(32) Nilges, M.; Kuszewski, J.; Brunger, A. T. *Computational Aspects of the Study of Biological Macromolecules by NMR*; Hoch, J. C., Ed.; Plenum Press: New York, 1991.

this last refinement stage were 50 kcal/mol·Å^2 for distance restraints, 60 kcal/mol·rad^2 for dihedral restraints, 1 kcal/mol·Å^2 for planarity restraints,and 70 kcal/mol·Å^2 for hydrogen bond restraints. A switched electrostatic function with a distance-dependent dielectric constant and a switched Lennard−Jones van der Waals potential function were used in this last stage. The final ensemble of five structures was deposited to the PDB under the ID code 1FC8.

Results

Exchangeable Proton Spectra. The 1D imino proton spectrum reveals three downfield resonances, which confirm base pair formation in the stem. In addition, two peaks of unit integral intensity with large line widths were observed for the imino protons of dT5 and dT6. The terminal rG1 and loop dG8 imino resonances were not observed because of solvent exchange. In contrast to the results on the all-RNA hairpin of the same sequence, we detected no base pair formation between dG8 and dT5.[22] A two-dimensional NOESY spectrum in H_2O was used to assign the imino protons (data not shown). One notable feature was an NOE between the imino proton of dT5 (10.70 ppm) and the H5 proton of rC4 that revealed base stacking between rC4 and dT5.

The Ribose Strand. As expected, the sugar conformation of the ribose residues (other than rC4) was measured to be C3′ endo. This identification was based on the presence of strong intraresidue NOE cross-peaks between base protons H6/H8 and the sugar H3′ protons and H1′−H2′ coupling constants of <2 Hz (Table 1). For residue rC4, the H6−H3′ NOE was slightly less intense, the H6−H2′ NOE more intense, and the H1′−H2′ *J*-coupling was 3 Hz.

PSEUROT calculations for residues rG1 and rG2 confirmed the C3′ endo sugar conformation (Table 1). A pseudorotation phase angle of ∼40° was calculated for rC4. For rA3, a number of sugar coupling constants were missing as a result of resonance overlap, and PSEUROT calculations could not be carried out. However, on the basis of the similarity of rG2 and rA3 cross-peaks in NOESY and DQF−COSY spectra, we can safely infer a C3′ endo sugar pucker for rA3.

The sequential NOE intensities were very characteristic of an A-type helix, as observed in RNA duplexes.[26] Strong (*n*)-H2′−(*n* + 1)H6/H8 sequential NOEs, typical of RNA and the ribose strand of RNA/DNA hybrid duplexes,[7−10] were observed in the 2′F-ANA/RNA stem; these sequential distances were measured to be 2.6 Å on average. An interstrand NOE was also detected between H2 of rA3 and H1′ of aF-C11.

H3′−P coupling constants for the first three phosphorus atoms were 9−10 Hz (Table 1). From the Karplus equation for H−C−O−P couplings,[33] this corresponds to four possible ϵ-angles, one of which is 220°. In the RNA strand of DNA/RNA hybrid structures, the ϵ-angle has been reported to be 180−240°.[8,11,13,15] This is consistent with an ϵ-angle of 220° in our hairpin. We observed weak couplings for both H5′−P and H5″−P, implying β-angles of 180°.[33]

The Deoxyribose Loop. Except for residue dT5, DNA sugar puckers were *south*. For all four residues, characteristic strong intraresidue H6/H8 to H2′ NOEs, weak H6/H8 to H3′ NOEs, and large H1′−H2′ scalar couplings were observed. For residue dT5, PSEUROT analysis revealed a mixture of C3′ endo and C2′ endo puckers with a predominance of the north conformer. The dT5 intrasugar H2" to H4′ NOE was also significantly stronger than what would have been expected from a uniquely C2′ endo conformation. In contrast, in the all-DNA hairpin studied by James et al.,[23] dT5 adopts primarily a south sugar pucker. This difference in the 2′F-ANA/RNA hairpin could be a result of the influence of the N-type sugars in the preceding ribose strand.

As opposed to the relatively static ribose residues, the loop residues showed significant dynamics. The H5−H6 NOE build-up curves for C7 (in the loop) and C11 (in the stem) were significantly different. No single loop structure was found that could satisfy all of the measured NOEs. For residues rC4−dT5, many sequential NOEs were observed that were consistent with dT5 stacking on rC4, as observed in the all-DNA hairpin of the same sequence.[23] Multiple sequential NOEs were also found between dT5 sugar protons and dT6 base protons. This indicates some stacking between dT5 and dT6, which is also observed in the all-DNA hairpin.[23] No strong or medium sequential NOEs were found between dC7 and dT6 or between dC7 and dG8; however, a medium-weak NOE between dC7 H5 and dT5 H2′ was observed, which is inconsistent with stacking of dT5 and dT6. Therefore, we conclude that the loop assumes multiple conformations in fast exchange on the NMR time scale. As a consequence, loop NOE restraints were relaxed to include larger error bounds for the calculation of the hairpin structure (see Experimental Section).

The loop β-angles were found to be trans on the basis of the small P−H5′ and P−H5″ coupling constants. P−H3′ coupling constants were found to be of medium intensity for dT5, dT6, and dC7 (Table 1). For dG8, the P−H3′ coupling constant was 3 Hz. This subtle difference may contain significant structural information but taking into account the high mobility of the loop, ϵ-angles were simply constrained as 240 ± 100° to avoid the sterically unfavorable gauche$^+$ angle.

2′-Fluoroarabinose Strand. The sugar conformation observed in residues 9−11 was O4′ endo. NOESY spectra revealed intraresidue H1′ and H4′ distances of only 2.35 Å (Figure 2). This could not be due to an equilibrium between C2′ endo and C3′ endo sugar puckers, because in both conformations, the H1′−H4′ distance is ∼3.3 Å. The observed 2′F-ANA distances are shorter than the reported distances, 2.6−3 Å, in the DNA strand of DNA/RNA duplexes.[8,14]

Vicinal ^{1}H−^{1}H coupling constants are determined not only by torsion angles but also by the presence of electronegative substituents. In the case of 2′F-ANA sugars, the presence of the fluorine atom decreases the size of the H1′−H2′ and H2′−H3′ scalar couplings. We used PSEUROT to predict sugar puckers of the 2′F-ANA strand by including appropriate electronegativity and orientation terms for the fluorine substituent on C2′.[28,29] In agreement with the NOE data, we found a predominantly east conformation for residues aF-G9, aF-T10 and aF-C11 (Table 1). The terminal aF-C12 residue displayed considerable mobility; the H1′−H4′ NOE (corresponding to 2.5 Å) indicated a partial O4′ endo conformation and the PSEUROT calculation revealed that the C3′ endo conformation was also highly populated.

In the 2′F-ANA strand, very strong sequential (*n*)H2′ to (*n* + 1)H6/H8 NOEs equivalent to 2.3 Å were observed. This is characteristic of B-form helices and was also observed in the DNA strand of a DNA/RNA hybrid duplex.[8] For residues 10−12, small H4′−H5′/5″ couplings were observed, implying gauche$^+$ γ torsion angles.

Except for aF-G9, the β-angles were found to be in the trans configuration on the basis of the symmetry and low intensity of the P−H5′/H5″ cross-peaks in the HP−HETCOR spectrum. For aF-G9, a very strong coupling was detected between the phosphate and one of the 5′ protons. This is the result of a gauche$^+$ or gauche$^-$ β-angle. Because of this ambiguity, we

(33) Kim, S. G.; Lin, L. J.; Reid, B. R. *Biochemistry* **1992**, *31*, 3564−3574.

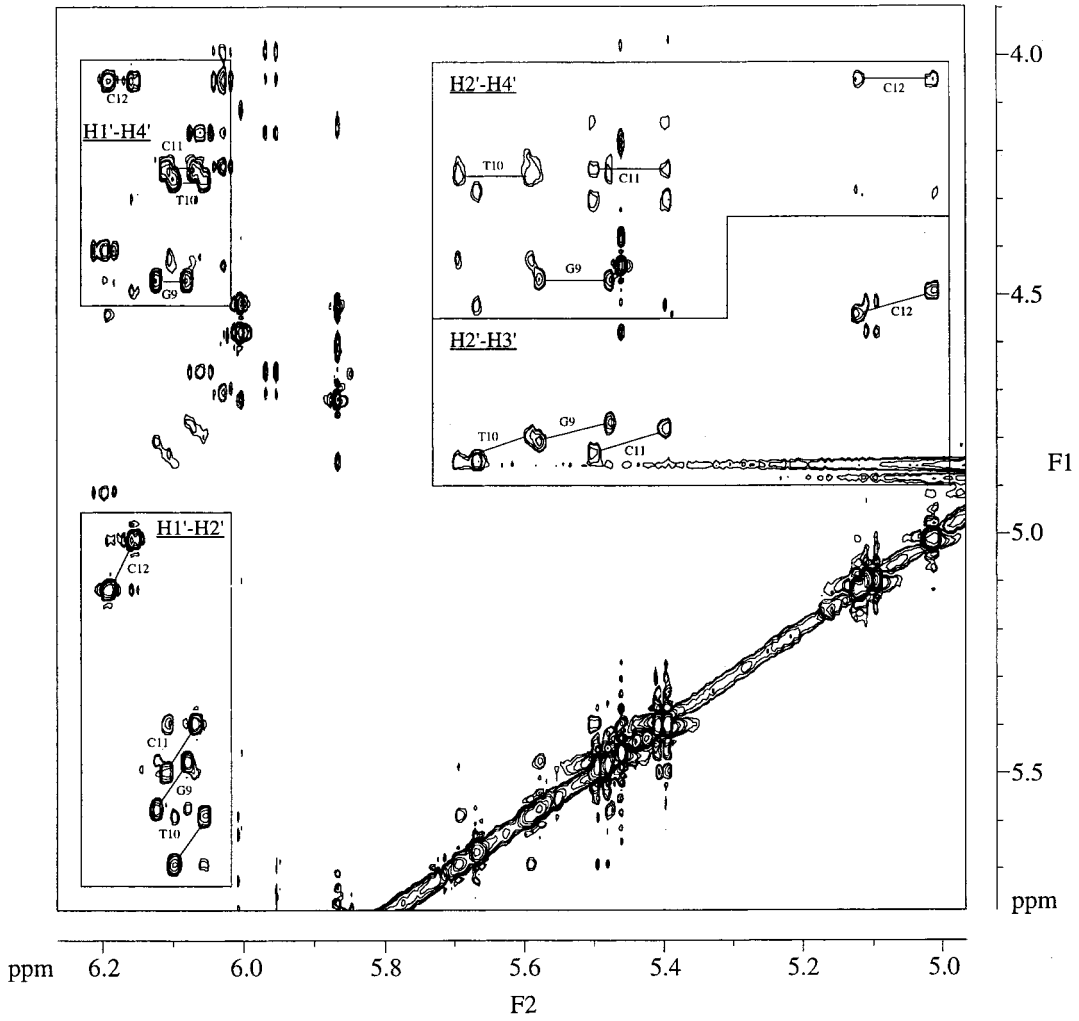

Figure 2. NOESY spectrum (200 ms) of the 2′F-ANA H1′/H2′/H3′/H4′ sugar protons. Four regions are identified according to the protons involved in NOE peaks. The H1′−H4′ NOEs are almost as intense as the H1′−H2′ NOEs (compare these with the H2′−H3′ and H2′−H4′ cross-peaks) and correspond to interproton distances of 2.35−2.5 Å. A similar pattern was observed at 50 ms.

did not restrain this angle in the structure calculations. P−H3′ coupling constants in the 2′F-ANA strand were significantly smaller than those in the RNA strand (Table 1). ϵ-angles derived from these couplings could be either 190 or 290°.[33] On the basis of literature data on DNA/RNA duplexes,[8,11,13,15] we restrained the ϵ-angles to 190°.

^{19}F NMR. This fluorine isotope is a spin = 1/2 nucleus and shows *J*-coupling to adjacent protons. Geminal coupling constants of ∼50 Hz (Table 2) were observed between F2′ and H2′. These values are typical for sugar rings with a fluorine substituent.[34] Vicinal coupling constants to H1′ and H3′ were between 20 and 27 Hz.

Unusual five-bond couplings were observed between the 2′F-ANA H6/H8 protons and fluorines. These have been previously observed in free mononucleotides.[19,35] There are two possible origins for this coupling: either the coupling is propagated through five bonds or there is a through-space electronic interaction between the two nuclei.[36] Theoretical and other NMR studies support the latter hypothesis.[36−41]

Structural Analysis. Simulated annealing was used to calculate the structure using 226 distance and 103 torsion angle restraints. From 68 initially converged structures, 5 were selected for final refinement using a more complete force field that included electrostatics (Figure 3). No structure had NOE violations > 0.1 Å or dihedral angles violations >10°. The all-atom RMSD for 2′F-ANA/RNA duplex residues is 0.33 Å. Inclusion of the loop in the superimposition raises the RMSD to 1.26 Å, but the stem residues remain closely superimposable, with an RMSD of only 0.50 Å. Loop residue dT5 is well-defined, with an RMSD of 0.64 Å, but the other loop residues, dT6, dC7, and dG8, were disordered with large RMSD values of 2.60, 3.62, and 1.71 Å, respectively.

Backbone torsion angles for stem residues are shown in Figure 4. The α-angles show convergence, despite the fact that they were not directly restrained. The values differ for the two strands, but they are all gauche$^-$ and close to values observed

(34) Barchi, J. J., Jr.; Jeong, L. S.; Siddiqui, M. A.; Marquez, V. E. *J. Biochem. Biophys. Methods*; **1997**, *34*, 11−29.
(35) Wright, J. A.; Taylor, N. F.; Fox, J. J. *J. Org. Chem.* **1969**, *34*, 2632−2636.
(36) Bergstrom, D.; Swartling, D. J.; Wisor, A.; Hoffmann, M. R. *Nucleosides Nucleotides* **1991**, *10*, 693−697.
(37) Barchi, J. J. J.; Marquez, V. E.; Driscoll, J. S.; Ford, H., Jr.; Mitsuya, H.; Shirasaka, T.; Aoki, S.; Kelley, J. A. *J. Med. Chem.* **1991**, *34*, 1647−1655.
(38) Herdewijn, P.; van Aerschot, A.; Kerremans, L. *Nucleosides Nucleotides* **1989**, *8*, 65−96.
(39) Marquez, V. E.; Lim, B. B.; Barchi, J. J., Jr.; Nicklaus, M. C. *Nucleosides and Nucleotides as Antitumor and Antiviral Agents*; Plenum Press: New York, 1993; pp 265−284.
(40) Kawasaki, A. M.; Casper, M. D.; Freier, S. M.; Lesnik, E. A.; Zounes, M. C.; Cummins, L. L.; Gonzalez, C.; Cook, P. D. *J. Med. Chem.* **1993**, *36*, 831−841.
(41) Wasylishen, R. *J. Am. Chem. Soc.* **1975**, *97*, 4545.

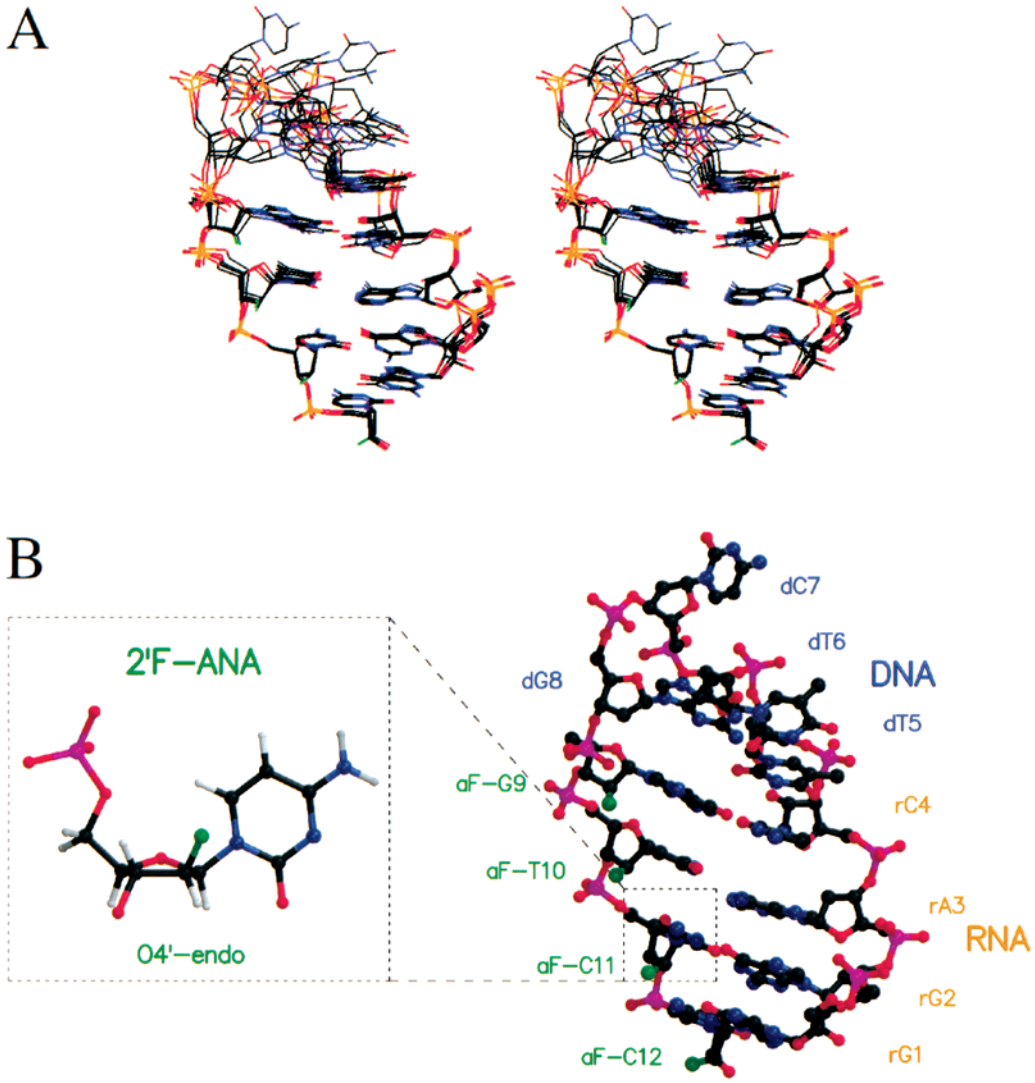

Figure 3. Structure of the oligonucleotide hairpin r(GGAC)d(TTCG)2′F-a(GTCC). (a) Stereoview of five structures aligned using the stem (PDB accession 1FC8). The duplex is very well defined, with an RMSD deviation of only 0.33 Å. In contrast, the loop is disordered, except for residue dT5, which stacks on rC4 in all five of the structures. (b) Single hairpin structure with detail of aF-C11 showing the O4′ endo sugar conformation. The fluorine atom (green), above the ring, is pseudoaxial and gauche with respect to the ring oxygen O4′. In the 2′F-ANA strand, fluorine−H6/H8 distances ranges between 2.6 and 2.8 Å, which engenders a small through-space coupling.[19,35,41]

in DNA/RNA duplexes in solution.[8,11,13] Similarly, ζ-angles were similar to literature values for DNA/RNA duplexes.

The stem χ-angles were very well defined, especially for the residues in the middle of the stem. Both of the strands show bases in the anti configuration, with values somewhat closer to 180° for the RNA residues. Similar values were observed in DNA/RNA duplexes,[8,11] although the range of angles was larger in the DNA strand of González et al.[11]

The program CURVES[42] was used to determine helical parameters for stem residues, which are shown in Table 3. Although the stem is short, the rigidity of the stem enabled us to calculate those parameters and compare them with literature data. Table 3 presents the structural parameters that best reflect the differences between the two canonical A-form and B-form helices.[43,44] Values reported in the literature differ significantly, and their magnitude seems to depend on sequence composition, computational aspects of the structure determinations, and the method used to determine the helical parameters.[8,11−14]

X-displacement values show small standard deviations and are between those of A- and B-DNA. This parameter is often reported to be slightly higher in DNA/RNA hybrids, although similar average values were found in the MD-tar ensemble calculated by González et al.[11] and single structure refinement of rR10/dY10 by Gyi et al.[13] The 2′F-ANA/RNA inclination also has intermediate values, although standard deviations are larger but still fall within the extreme values of A-form and B-form duplexes. Similar values were observed in DNA/RNA duplexes.[8,11−14] Interbase helical parameters show good standard deviations, that is, they are well-defined and in general agreement with values for DNA/RNA hybrids. Only the rG2−rA3 base pair rise has a value intermediate between that of A-form and B-form duplexes.

The minor groove width was obtained by subtracting 5.8 Å from the smallest interstrand P−P distance. Two distances (P12−P4 and P11−P5) were used for this measurement, and results are shown in Table 3. Although P5 belongs to a loop residue, dT5 forms a continuation of the RNA strand helicity,

(42) Lavery, R.; Sklenar, H. *Curves 5.2, Helical Analysis of Irregular Nucleic Acids*; Laboratoire de Biochimie Theorique, CNRS URA 77: Paris, France, 1997.
(43) *Sybyl 6.5, Update #2*; Tripos Inc.: 1999.
(44) Saenger, W. *Principles of Nucleic Acid Structure*; Springer-Verlag: New York, 1984.

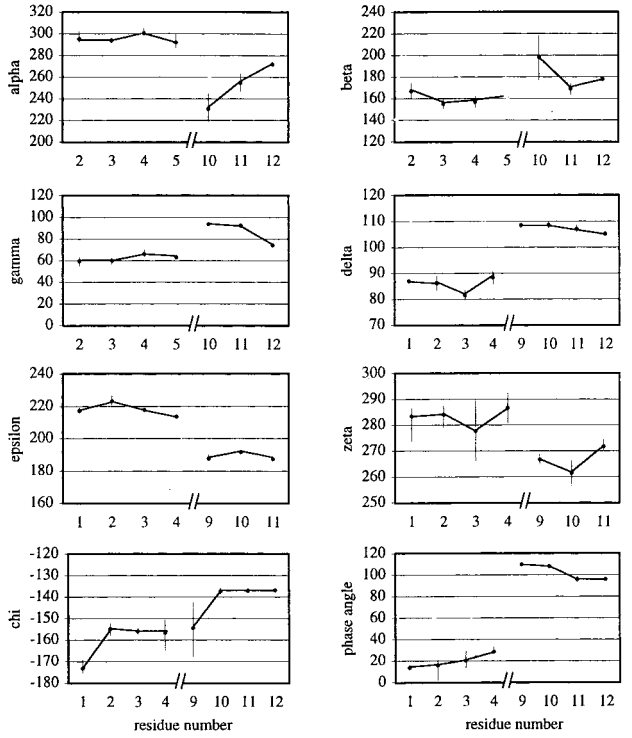

Figure 4. Backbone glycosidic torsion angles and pseudorotation phase angles for stem residues from the five structures produced by simulated annealing. Angles are reported in degrees and residues are numbered 5′ to 3′. The continuous lines indicate average angles and the vertical bars indicate the maximum and minimum values.

Table 3. Selected Structural Parameters for the Stem Residues and Comparison to Parameters Calculated for Canonical Forms[a]

base pair/axis and base/base helical parameters				minor groove width Å	
	xdisp Å	inclination deg	propel deg	P12−P4[b]	P11−P5
G1−C12	−2.8 (0.3)	4.7 (2.0)	−6.3 (3.8)		
G2−C11	−3.0 (0.2)	7.3 (2.5)	−11.2 (3.7)	9.3 (0.2)	8.3 (0.7)
A3−T10	−3.0 (0.2)	5.5 (2.8)	−5.5 (3.3)		
C4−G9	−3.0 (0.3)	6.9 (3.4)	−5.6 (5.5)		
A-DNA	−5.4	19.3	13.2	11.1	
B-DNA	−0.7	−5.9	4.0	5.9	

Inter-base pair helical parameters			
	slide, Å	rise, Å	twist, deg
G1−G2	−1.9 (0.3)	3.7 (0.4)	32.0 (1.8)
G2−A3	−1.7 (0.4)	3.0 (0.3)	35.5 (2.6)
A3−C4	−2.0 (0.3)	3.4 (0.4)	31.1 (2.0)
A-DNA	−2.1	2.6	32.7
B-DNA	−0.8	3.4	36.3

[a] All parameters were calculated using the program CURVES. Average value and standard deviation in brackets are shown for all parameters. Global values were used for all parameters, except for local slide. [b] Numbering correspond to residue number, with phosphate in 5′ position.

which justifies the choice of the P11−P5 as a second indicator of the groove width. Significantly, the minor groove widths of 2′F-ANA/RNA and DNA/RNA are very similar (8−10 Å) and are intermediate between those measured for A-form and B-form duplexes.[8,11,12,14]

Discussion

Since their development over 20 years ago, antisense drugs have been a major area of interest in medicinal chemistry.[45] 2′F-ANA oligonucleotides meet three important criteria as potential antisense agents. The first, revealed by thermal denaturation studies, is enhanced affinity for complementary RNA targets. 2′F-ANA/RNA hybrid duplexes have melting temperatures roughly 1 °C/bp higher than homologous DNA/RNA hybrid duplexes.[19] Further, analysis of mismatched duplexes shows that 2′F-ANAs maintain specificity in complement strand recognition. The second criterion is activation of RNase H to hydrolyze the target RNA strand. 2′F-ANA/RNA hybrids efficiently carry out this process and are an important advance over a number of modified oligonucleotide technologies that lead to stable duplexes but fail to activate RNase H. Finally, antisense oligonucleotides need to show increased nuclease resistance in order to increase their efficacy and longevity. 2′F-ANA shows enhanced stability against snake venom phosphodiesterase and is more stable than DNA and 2′F-RNA.[46] These results suggest that 2′F-ANA (and its derivatives) may serve as leads in the design of new antisense therapeutics as well as provide tools for studying and controlling gene expression in conditions for which membrane permeability is not an issue.

There are few structural studies of nucleic acids with fluoroarabinonucleotides. The crystal structure of DNA with 2′-deoxy-2′-fluoro-β-D-arabinofuranosyl thymines has been reported.[16] These residues adopt the O4′ endo conformation, as in the 2′F-ANA strand of our hairpin. Venkateswarlu and Ferguson[21,47] studied, by computational methods, the effects of C2′-substitution on arabinonucleic acids conformation. They found that these fluoro-substituted arabinose sugars adopt a south-like conformation but tend toward O4′ endo. They calculated the conformation of the 2′F-ANA/RNA hybrid duplex. Helical parameters and backbone torsion angles are generally in agreement with those found in the present study. Recently, a theoretical model of a 2′F-ANA/RNA hybrid duplex was derived from the X-ray structure of a DNA duplex with incorporated [3.3.0]bicyclo-ANA.[20] This conformationally restricted arabinose analogue also exhibits an O4′ endo conformation. The structure of these incorporated nucleotides was used to generate the 2′F-ANA strand of the model hybrid duplex. The structural characteristics of the hypothetical hybrid duplex are similar to those that are calculated by Venkateswarlu and Ferguson.[21,47] However, it should be noted that bc-ANA does not elicit RNase H activity,[20] so that steric considerations also have to be considered when designing oligonucleotides as substrates for RNase H.

Different mechanisms have been proposed as to how RNAse H distinguishes hybrid duplexes from pure DNA or RNA duplexes. Fedoroff et al.[8] hypothesized that discrimination is based on the difference in minor groove width, which is dependent on the conformation of both strands. NMR titration studies have identified Cys13, Asn44, Asn16, and Asn45 as critical residues involved in RNase H residues' binding to the hybrid duplex.[8] Fedoroff et al. proposed that the first two residues make hydrogen bonds with 2′-OH groups in the RNA strand, and Asn16 and Asn45 are hydrogen-bonded to phosphodiester oxygen atoms in the DNA backbone, across the minor groove, emphasizing the importance of the minor groove width. In the 2′F-ANA/RNA stem of our hairpin molecule, an intermediate minor groove width was also obtained. On the basis of the proposed mechanism of RNase H action, we would, therefore, expect the 2′F-ANA/RNA hybrid duplex to be a

(45) Zamenick, P. C.; Stephenson, M. L. *Proc. Natl. Acad. Sci. U.S.A.* **1978**, *75*, 280−284.

(46) Noronha, A. M.; Wilds, C. J.; Lok, C. N.; Viazovkina, K.; Arion, D.; Parniak, M. A.; Damha, M. J. *Biochemistry* **2000**, *39*, 7050−7062.

(47) Venkateswarlu, D.; Lind, K. E.; Mohan, V.; Manoharan, M.; Ferguson, D. M. *Nucleic Acids Res.* **1999**, *27*, 2189−2195.

substrate for RNase H, as has been confirmed by enzymatic assays using several 18 bp 2′F-ANA/RNA hybrid duplexes.[6,24]

Other hypotheses for the basis of RNase H discrimination have been proposed. Szyperski et al.[48] proposed an induced-fit model based on the flexibility of deoxyribose and on the hydration patterns of duplexes. According to their model, 2′F-ANA/RNA should not be a substrate for RNAse H, because the 2′F-arabinonucleotides are relatively rigid. It appears that DNA flexibility alone does not explain RNAse H recognition. Hsu et al.[49] retained the hydration pattern hypothesis in conjunction with the importance of the minor groove width. The characteristic pattern of hydration that is associated with the RNA strand, particularly with the C2′-OH group, as well as with the particular geometry and size of the minor groove and the average position of the phosphate groups on the strand complementary to RNA, may dictate overall RNAse H specificity.

As initially hypothesized, the fluoroarabinonucleotides mimic quite closely the deoxyribonucleotides when bound to the RNA strand.[6] Furthermore, the fluoroarabinose nucleotides are much more rigid than deoxyribose. The energy barrier for interconversion between sugar conformers is higher because of the large gauche effect from the strongly electronegative fluorine atom and the furanose ring oxygen (O4′). As a consequence, the thermodynamic stability of a 2′F-ANA/RNA double helix is higher than for a DNA/RNA double helix, as a result of the preorganization of the 2′F-ANA residues, which entropically favors a double helix formation.[6,16,50]

There is considerable debate concerning the sugar puckers' conformation in the DNA strand of DNA/RNA hybrid duplexes; Reid and colleagues first proposed that DNA sugar puckers adopt the O4′ endo conformation,[8,10,12] but the work of Brown and James supports a C2′ endo to C3′ endo equilibrium model.[9,11,13] On the basis of our work on the 2′F-ANA/RNA duplex, we suggest that the DNA strands in DNA/RNA hybrids should be modeled as a mixture of three conformers: C2′ endo, C3′ endo, and O4′ endo. In the case of 2′F-ANA/RNA, both NOE ($d_{H1'-H4'} = 2.35$ Å) and *J*-coupling data imply the existence of a single O4′ endo sugar pucker for the antisense strand. We note that if $d_{H1'-H4'}$ is ∼2.6 Å, as observed in the DNA strand of a DNA/RNA hybrid,[8] only 40% O4′ endo is necessary to yield this average NOE distance (Figure 5). If one assumes a three-conformer equilibrium model, the remaining 60% can be any mixture of C2′ endo and C3′ endo to account for the observed scalar couplings. In the case of the terminal 2′F-ANA/RNA residue, aF-C12, we measured 55% of O4′ endo conformer, on the basis of the observed $d_{H1'-H4'}$ distance of 2.5 Å (from the NOE cross-peak intensity at short mixing times). This is in excellent agreement with the PSEUROT result of ∼50% O4′ endo that is based on scalar couplings (Table 1).

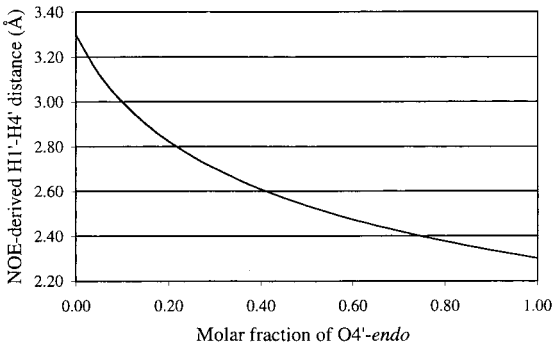

Figure 5. Average H1′−H4′ distance calculated as a function of averaging in a three-state model of C2′ endo, C3′ endo and O4′ endo sugar conformers. Because the H1′−H4′ distance is the same for both C2′ endo and C3′ endo (3.3 Å), the measured H1′−H4′ NOE at short mixing times in the absence of spin diffusion can be used as a direct measure of the mole fraction of O4′ endo sugar pucker. The experimentally measured distance (in Å) was calculated assuming $1/r^6$ NOE averaging as $d_{H1'-H4'} = [x(2.3)^{-6} + (1 - x)(3.3)^{-6}]^{-1/6}$, where x is the molar fraction of O4′ endo.

Although not the central theme of this paper, the structure of the loop is quite interesting. It is less well structured than in the all-RNA homologous hairpin, where the loop is stabilized by an inverse Wobble base pair.[22] The structure is more similar to that of the all-DNA hairpin, where the same stacking between C4 and T5 occurs.[23] This stacking probably helps to stabilize the sharp turn in the backbone and lower the energy of formation of the hairpin. On the basis of the differences in the RNA and DNA loops, it appears that the chemical composition of the loop is the most important factor for determining the loop structure. When composed of deoxyribose sugars, the loop is very flexible, with minimal effects on the conformation of the stem.

In conclusion, we have shown that a 2′F-ANA/RNA duplex adopts a structure that mimics a DNA/RNA hybrid duplex. The 2′F-ANA sugars are O4′ endo and conformationally rigid, which may explain the increased stability of 2′F-ANA/RNA duplexes. Finally, the NMR studies described here support the notion that activation of RNase H requires a DNA-like oligonucleotide that forms a duplex with an intermediate minor groove width.

Acknowledgment. We thank Phil Williams for use of the Bruker DRX300 spectrometer at the National Tritium Labeling Facility (Lawrence Berkeley Natl. Laboratory) and Steven Laplante for use of the DRX400 at Bio-Méga/Boehringer-Ingelheim (Laval, Québec). This work was supported by NSERC and MRC grants to Masad Damha and Kalle Gehring.

Supporting Information Available: One table containing the chemical shifts of ^{1}H, ^{19}F, and ^{31}P resonances referenced to DSS, trifluoroacetic acid, and phosphoric acid, respectively, and a 300 MHz ^{1}H−^{19}F 2D correlation spectrum used to assign fluorine resonances (PDF). This material is available free of charge via the Internet at http://pubs.acs.org.

JA003859P

(48) Szyperski, T.; Götte, M.; Billeter, M.; Perola, E.; Cellai, L.; Heumann, H.; Wütrich, K. *J. Biomol. NMR* **1999**, *13*, 343−355.

(49) Hsu, S.-T.; Chou, M.-T.; Cheng, J.-W. *Nucleic Acids Res.* **2000**, *28*, 1322−1331.

(50) Wilds, C. J.; Damha, M. J. *Bioconjug. Chem.* **1999**, *10*, 299−305.